T. Kowalewski

INTERNATIONAL UNION OF THEORETICAL AND APPLIED MECHANICS

TOPOLOGICAL FLUID MECHANICS

Proceedings of the IUTAM Symposium

Cambridge, UK 13–18 August 1989

Edited by H. K. MOFFATT and A. TSINOBER

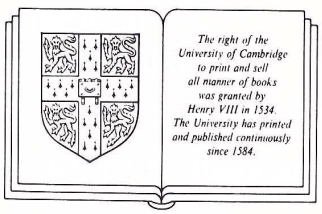

CAMBRIDGE UNIVERSITY PRESS
Cambridge
New York Port Chester
Melbourne Sydney

Published by the Press Syndicate of the University of Cambridge
The Pitt Building, Trumpington Street, Cambridge CB2 1RP
40 West 20th Street, New York, NY 10011, USA
10 Stamford Road, Oakleigh, Melbourne 3166, Australia

First published 1990

Printed in Great Britain at the University Press, Cambridge

British Library cataloguing in publication data

Topological fluid mechanics: proceedings of the IUTAM Symposium, Cambridge UK, 13–18 August 1989.
1. Western bloc countries. Imports from Soviet Union: Natural gas & petroleum. Politico–economic aspects
I. International Union of Theoretical and Applied Mechanics II. Moffatt, H. K. III. Tsinober, A.
532.'001'51

ISBN 0–521–38145–2

Library of Congress cataloguing in publication data available

ISBN 0 521 38145 2

International Committee

V.I. ARNOL'D	USSR
U. DALLMANN	FRG
U. FRISCH	France
P. GERMAIN (President IUTAM)	France
H. HASIMOTO	Japan
F. HUSSAIN	USA
H.K. MOFFATT (Chairman)	UK
E.N. PARKER	USA
A.E. PERRY	Australia
A. TSINOBER	Israel

Local Organising Committee

H.K. MOFFATT (Chairman)
K. BAJER
R.E. BRITTER
D.G. DRITSCHEL
M. GASTER
P.H. HAYNES
J.C.R. HUNT
SARAH KIRKUP (Secretary)
A.J. MESTEL
M.R.E PROCTOR
W.E. WARD

This Symposium was sponsored by the International Union of Theoretical and Applied Mechanics, with additional financial support which is gratefully acknowledged from the following organisations:

- The Royal Society
- The London Mathematical Society
- Trinity College Cambridge
- US Air Force European Office of Aerospace Research and Development (EOARD)
- Office Naval Research Europe (ONREUR)
- ALCAN International Ltd.
- British Aerospace plc
- Cambridge Environmental Research Consultants Ltd.
- ICI Engineering
- Rolls Royce plc
- Schlumberger Cambridge Research Ltd.

Experimental and Numerical Investigation of Natural Convection in a Cube with Two Heated Side Walls

W.J. HILLER[1], ST. KOCH[1], T.A. KOWALEWSKI[1], G. DE VAHL DAVIS[2] & M. BEHNIA[2]

[1]Max-Planck-Institut für Strömungsforschung, Göttingen, FRG
[2]University of New South Wales, Kensington, N.S.W., Australia

1 INTRODUCTION

Experimental knowledge of natural convection within enclosures is still far from complete. Even stationary convective flow in a square box with differentially heated side walls, a problem which at first view seems to be closely related to the corresponding two-dimensional case, exhibits an intricate three-dimensional structure. The experimental simulation of two-dimensional plane flows is always a compromise as additional walls are needed to prevent the medium from lateral escape. These walls in their turn induce three-dimensional motion, as has been discussed in [1]. Even if by proper design of the size of the box the influence of these walls can be kept small in the centre region of the enclosure, the topological structure of the flow field is fundamentally changed. Problems like separation, stability of flow configurations, and onset of oscillatory motion can be discussed only by taking into account the three-dimensional character of the flow field [2].

Therefore, it appears quite useful to perform supplementary experiments to collect more details on the flow structure. For this purpose, a cube shaped box with two opposite, vertical walls kept at different temperatures and the other walls kept adiabatic appears very suitable, as a pronounced three-dimensional behaviour of the flow field is to be expected.

It has been already revealed in a former study [3] that the flow structure away from the vertical mid-plane of the cavity is strongly three-dimensional and, for the liquid used in that study, asymmetrical, and differs strikingly from existing two- and three-dimensional numerical results. At relatively low Rayleigh numbers ($Ra < 6 \cdot 10^4$) the core of the spiral vortex transporting fluid from the front and back walls (i.e. the adiabatic vertical walls) to the centre of the cavity is concave with respect to the heated wall. At increasing Rayleigh number a second spiral vortex twists off from the first vortex at approximately half the distance between the front and back walls and the centre of the cavity.

These effects may be due to failure to achieve a true adiabatic condition on the insulating vertical walls and are certainly affected by the temperature-dependent viscosity of the liquid. Unfortunately, there exist neither transparent fluids of constant material properties which are suited for liquid crystal tracers nor transparent, ideally adiabatic walls

which are needed for the purpose of observation. Therefore, the experiments have to be accompanied by a numerical procedure able to take into account the experimental conditions, as most of the theoretical treatments of convective flow known to us have been performed by assuming a constant property Boussinesq fluid and ideal isothermal or adiabatic walls.

The present paper is a preliminary combined experimental and numerical study of three-dimensional natural convection aimed at revealing details of the flow structures, especially for higher Rayleigh numbers. The discrepancies between the observed flow structures and prior numerical results are under numerical investigation with respect to wall heat losses and the temperature dependence of the fluid properties.

2 DESCRIPTION OF THE PROBLEM

We consider the convective flow in a cubic box filled with a viscous heat-conducting liquid. The fluid viscosity and density are assumed to be only temperature dependent. Two opposite, vertical walls of the cube are isothermal at temperatures T_h (hot) and T_c (cold), respectively. The four other walls are isolators of finite thermal diffusivity α_w. Due to temperature gradients existing between the fluid inside the cavity and the surrounding atmosphere and also along the front and back walls, lid and floor of the box, a heat flux both through and along the walls comes into existence.

The origin of a rectangular Cartesian coordinate system is placed at an upper corner of the box as illustrated in Fig.1. Two non-dimensional parameters are chosen to compare the numerical and experimental results:

Rayleigh number,

$$(1)\quad Ra = \frac{g \cdot \beta \cdot d^3 \cdot (T_h - T_c)}{\alpha \nu}$$

and the Prandtl number,

$$(2)\quad Pr = \nu/\alpha \ .$$

In the above definitions, $g, d, T_h, T_c, \alpha, \beta, \nu$ denote gravitational acceleration, cavity dimension, vertical wall temperatures, thermal diffusivity, coefficient of thermal expansion and kinematic viscosity, respectively.

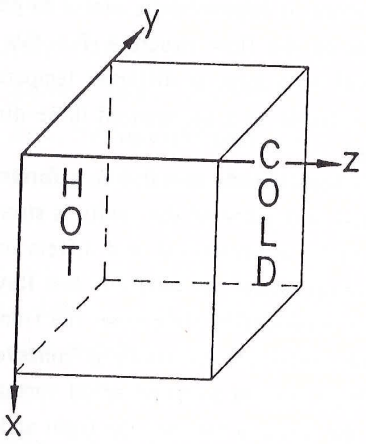

Fig. 1. The cube shaped enclosure and coordinate orientation. Hot wall at z = 0, cold wall at z = 1.

3 EXPERIMENTAL

3.1 Apparatus and Procedure

The apparatus used in the experiment is essentially the same as that used previously [3]. The convection cavity consists of a tube of square cross-section of internal dimension and length 38mm made from 8 mm thick Plexiglas. Both ends of the tube are closed with a black anodized copper plate of 60mm by 60mm, and 50mm thick. Each of these plates is maintained at constant temperature by a water flow which passes through internal passages in the plates. The temperature of the water is controlled by a thermostat. The temperature difference between the two walls was varied in the range from 2.5°C to 18°C, whereas the mean temperature was kept at approx. 27°C. The temperatures were measured continuously by means of thermocouples and recorded by a Philips multichannel recorder. The temperature fluctuations with time observed on the end plates were below 0.1°C. The room temperature was measured to be 22 ± 1°C.

The Rayleigh numbers ranged from 10^4 to 10^6. Aqueous solutions of glycerol of various concentrations were employed as flow media. The Prandtl number varied from 6900 (pure glycerol) to approximately 200 for a 70% glycerol-water mixture. Temperature and velocity fields were measured with help of liquid crystals suspended as small tracer particles in the liquid [3]. The visualization of temperature using liquid crystals is based on their temperature-dependent refractivity for the wavelength (colour) of visible light. If they are illuminated with white light, then the colour of the light reflected from the liquid crystals changes from red to blue if the temperature is raised (in a well defined temperature range which depends on the type of LC used). The flow was observed at different vertical (z-x) and horizontal (y-z) cross sections of the cavity using a light sheet technique.

3.2 Flow Structure

At first view, a characteristic unicellular flow pattern similar to the two-dimensional case is observed at moderate Rayleigh numbers < $6{\cdot}10^4$ in the centre plane of the cavity (Fig. 2a), and the slope of the isotherms in the centre region of the channel is very small but still positive. The influence of the non-zero thermal conductivity of the top and bottom walls becomes visible by a deflection of the ends of the isotherms in such a way that close to these walls the z-component of the temperature gradient becomes more uniform. Estimates of the relative rates of heat transfer by convection to the surroundings and conduction along the Plexiglas walls suggest that this effect is due rather more to the latter than the former. The presence of the front and back walls induces axial flow components in the entire flow field with the result that the tracer particles in z-x planes no longer follow closed lines. They spiral outwards on the centre mid-plane of the cube and inwards in the neighbourhood of the front and back walls. Both regions are connected by a mean effective axial flow component which is directed to the centre of the cavity (for the inner region of the spirals) and to the front or back walls (for the

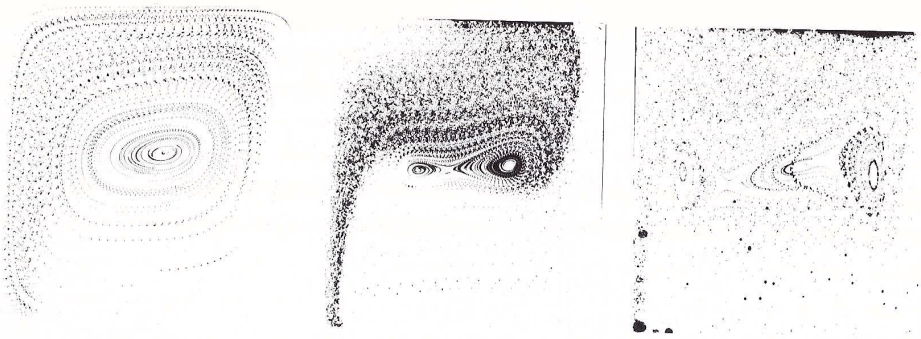

(a) (b) (c)

Fig. 2. B&W multiexposure photograph of the flow in the vertical centre plane (y = 0.5). Left side (z=0) is the hot wall; (a) Ra = $2 \cdot 10^4$, Pr = 6300; (b) Ra = $8 \cdot 10^4$, Pr = 6900; (c) Ra = $7.5 \cdot 10^5$, Pr = 225. See also colour plate, displaying additionally streamlines in a vertical plane y = 0.05. Red colour corresponds to~27^oC, blue to~29^oC.

outer region of the spirals). The ends of the spiral axis are shifted towards the heated side wall (Fig.3a). The flow field is symmetric with respect to the centre (y = 0.5) plane. If the Rayleigh number is raised above approximately $6.5 \cdot 10^4$ a negative slope of the isotherms appears in the middle region of the cubic enclosure which is caused by the increased convective heat transport (Fig.2b). As a consequence of the negative temperature gradient, the vortex splits up there into two vortices as in the two-dimensional case [4]. It seems as if part of the outer region of the original vortex twists off and forms a new spiral. Both spirals are clockwise when viewed in the direction of increasing y. For a Rayleigh number of 80,000 the points where the vortex splits are about midway between the centre vertical z-x plane and the front and back walls, respectively. On the front and back walls only one vortex is observed, and the slope of the isotherms is positive as is to be expected. Like in the one-vortex system the velocity component along the centre region of the two spirals is directed towards the vertical centre plane. There, the flow is deflected by an outward spiraling motion and finally returns back to the front wall and spirals inward. The temperature in the core of the spiral close to the cold wall is higher than the temperature in the core of the spiral close to the hot one. While the axis of the vortex near the hot wall is quite straight, the axis of the other one is considerably curved (Fig. 3b). Between these two configurations no hysteresis could be detected experimentally.

Further increase of the Rayleigh number results in a shift of the two vortices closer to the side walls z=0 and z=1, respectively, and the flow becomes strongly three-dimensional. This can be immediately deduced from the crossing of the particle traces visible in a vertical centre cross section when illuminated by a thin (2 mm) light sheet. The inner loops of the two spirals are strongly inclined with respect to the z-x plane in the

neighbourhood of the front and back walls. For Ra = $7.5 \cdot 10^5$ on each side between the centre plane and the walls a third vortex is observed. Its pitch is so large that for the visualization in the experiment thick light sheets have to be applied. Fig. 2c shows a vertical cross section at y = 0.4 illuminated by a light sheet of 5mm. All spirals are turning clockwise. In the vicinity of the cores of the two spirals close to the hot and cold walls, respectively, the flow direction along their axes shows inward and outward components. There exist ringshaped regions around the vortex cores in which the tracer particles stay for several revolutions as if they were trapped. The flow observed at horizontal plane x = 0.5 has close to the front and back walls dominating velocity component into these walls (Fig. 3c).

The largest Rayleigh number realized up to now is about $3.2 \cdot 10^7$. In this case, water was used as a flow medium in order to avoid too high temperature differences $T_h - T_c$. The flow is still stationary and on the vertical mid-plane the two aforementioned vortices are also observed, with these cores now being very close to the corresponding side walls.

4 NUMERICAL MODELING

In conjunction with the experimental programme, a numerical study of this problem has commenced. This involves the solution of finite difference approximations to the equations of motion and energy. Two computer codes are in use. In one, the thermal conductivity, viscosity and specific heat of the fluid are assumed to be constant, while in the other this restriction is removed: polynomial functions of temperature are used to represent these properties. However, in the temperature range where the experiments are performed only viscosity varies significantly with temperature. The functional description of this dependence was done by fitting the approximating function to the measured values of the viscosity of the working fluid. The thermal conductivity and specific heat of the fluid were kept constant in the present calculations.

In each code the Boussinesq approximation is made: the density is assumed constant except in the buoyancy term of the equation of motion.

The constant property equations are well-known (e.g. [1,5]) and need not be stated here. The variable property equations, containing derivatives of the fluid properties, are extremely lengthy and will not be given here. They can be found in [6].

Also in each code, the thermal boundary conditions are sufficiently flexible to allow the imposition of arbitrary temperature, specified heat flux or specified heat transfer coefficient boundary conditions on each of the six surfaces of the box. In the present study, the two heated side walls are assumed to be isothermal. The non-adiabatic boundary conditions of the remaining four non-isothermal walls were approximated by assuming a constant heat flux through each wall. This heat flux was estimated by using the theory for the heat transfer through a thick, infinite wide plane plate of uniform

conductivity into a gaseous environment. The ambient temperature was the room temperature (22°C). For the calculation of the heat flux coefficients the inner temperature of the wall was assumed to be constant. For the lid surface, this temperature was assumed to be T_h, for the floor surface T_c, and for the front and back walls $(T_h - T_c)/2$.

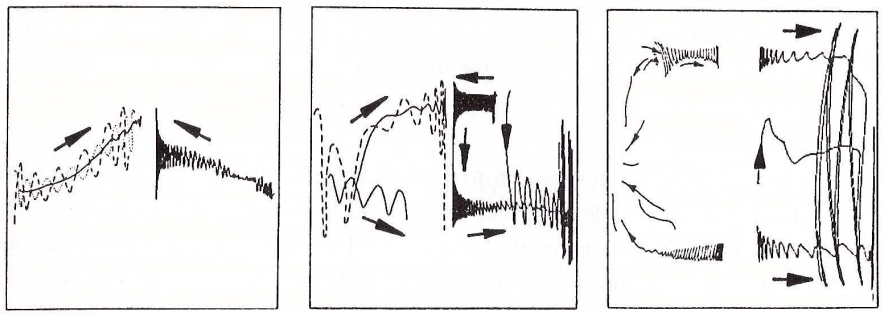

(a) (b) (c)

Fig. 3. Streamlines in the horizontal plane x = 0.5, left side of the figure - copied from the photographs, right - numerical simulation. (a) Ra = $2 \cdot 10^4$; (b) Ra = $8 \cdot 10^4$; (c) Ra = $7.5 \cdot 10^5$.

The two codes (variable and constant fluid properties) were developed for different purposes, but it is hoped that their parallel use in this work will enable a ready evaluation to be made of the effects of the temperature dependence of the fluid properties on the essential features of the flow. The motion of the fluid has been visualized from the computer solutions by the construction of particle tracks through the integration of the equations defining the velocity components (i.e., $\partial x/\partial t = u$, etc.) The validity of the tracks has been verified in a number of ways including reduction of the time step and a reversal of all velocities to enable the track to be traversed in reverse. Initially all solutions were computed on a 21 by 21 by 21 mesh, chosen as a compromise between accuracy and cost. This mesh has been shown to be sufficient to yield errors of less that 2% for natural convection in air at values of Rayleigh number up to 10^5 [7]. The present computations are done for a much higher Prandtl number (and therefore much thicker boundary layers). It is confidently believed, therefore, that this mesh is more that adequate if a global description of the flow is of interest. However, the localization of singularities appeared to be more sensible of the mesh size, especially at higher values of Rayleigh number. Increasing the mesh size (up to 51x51x51) several test runs of the constant properties code were done to check how far the mesh size influences the form of the calculated tracks. It was found that for Ra > $4 \cdot 10^4$ a finer mesh of 31 by 31 by 31 must be employed if the code is used to detect local flow structures.

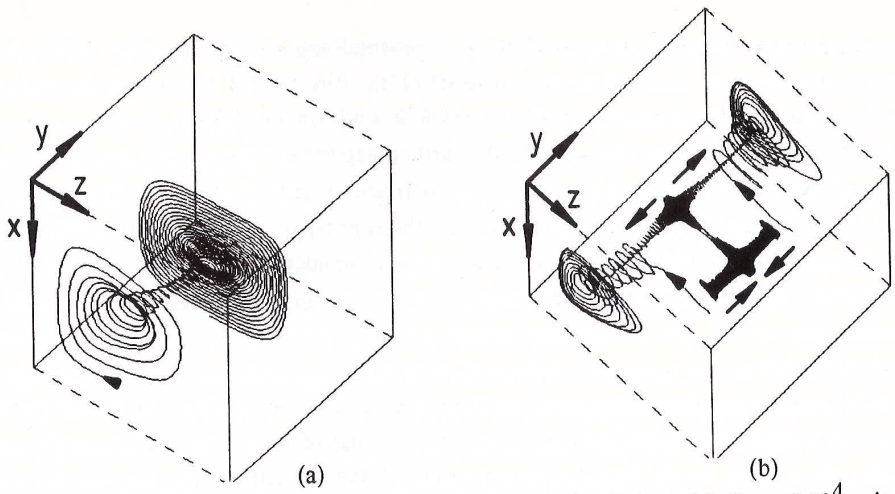

Fig. 4 Streamlines in perspective view - numerical simulation. (a) Ra = $2 \cdot 10^4$, single particle released near the front wall at the point (0.82,0.09,0.42); (b) Ra = $8 \cdot 10^4$, two particles released at the points (0.5,0.32,0.7) and (0.5,0.27,0.72) (other two released symmetrical to the centre plane y = 0.5). The first particle moves into the centre plane, then towards the hot wall and finally spirals towards the front wall. The second particle spirals directly to the front wall, merging with the spiral of the first one.

The variable viscosity of the fluid changes the symmetry of the flow with respect to the plane z = 0.5 (the flow at the hot side of the cavity is faster than at the cold one). Calculations performed with the variable property code give a very good quantitative description of the non-symmetrical velocity profiles in the centre region of the cavity (the calculated velocity components deviate within a few percent from the measurements reported in [3]). However, when comparing the tracks calculated with help of both codes it became obvious that the major influence on the flow structures is due to the thermal boundary conditions on the four non-isothermal walls, whereas variable fluid properties modify only slightly the calculated tracks. On the other hand, the huge storage needed for the variable property code limits (at the present time) its application to a 21x21x21 mesh. Therefore further numerical calculation were done with the constant property code, non-adiabatic thermal conditions on the side walls, and a uniform 31x31x31 mesh.

The preliminary numerical results which we have obtained reveal many of the same principal features of the flow: at low Rayleigh number, the movement of the fluid along a single spiral (Fig.4a) from the end walls (y = 0.1) towards the mid-plane (y = 0.5). Increasing Rayleigh number we observe a splitting of the single spiral into two in the region on either side of the mid-plane accompanying by a reversal of their direction. Also an additional singular point is detected for the spiral on the cold side of the cavity (Fig.4b). Such a point, observed in the experiments for higher Rayleigh number ($7.5 \cdot 10^5$), disappears in the numerical simulation made for this Rayleigh number.

There is a major discrepancy between the experimental and numerical results which we have not yet resolved: in the latter, the reversal of the direction of the spiral takes place at a Rayleigh number between 40,000 and 60,000 while in the former it has not been observed at 80,000 but at Ra = 750,000. Further experiments are being made in the intermediate range of Ra to identify the experimental critical value of Ra for this reversal. So far, we are unable to explain the discrepancy. Due to the unsolved experimental-numerical discrepancies we based our topological description of the flow exclusively on the experimental data.

5 DISCUSSION

The global topological structure of the one-vortex system (Ra = 20,000) is shown in Fig. 5a. The singularities in the corners and on the edges of the cube are either nodes or saddle points. They result from the v-component of the velocity generated by the front and back walls. Additionally on each of these walls there exists a focal point into which the streamlines from the wall spiral in, and on the vertical centre plane there is a third focal point from where the streamlines spiral out. The streamline connecting the front focal point with that of the centre plain shall only indicate that we have observed tracer particles which closely follow this path. For very low Rayleigh numbers there exist separation bubbles in the lower right front and back corners that disappear when the Rayleigh number increases.

The topological structure of the two-vortex system (Ra = 80,000) is shown in Fig. 5b. The singularities on the corners and the edges of the cube and those on the front and back walls remain unchanged, with exception of the singularity on the upper left edge where possibly a flow reversal occurs. In the center vertical plane two vortices are observed to which the two focal points separated by a saddle point correspond.

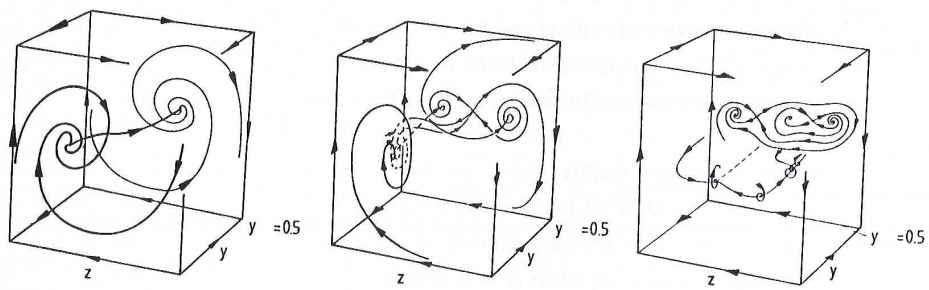

(a) (b) (c)

Fig. 5 Principal topological structure of the flow. Only the front half of the cube is displayed. (a) Ra = $2 \cdot 10^4$; (b) Ra = $8 \cdot 10^4$; (c) Ra = $7.5 \cdot 10^5$. (Arrows indicate the direction of streamlines).

The case where a third vortex becomes clearly visible ($Ra = 7.5 \cdot 10^5$) is at the moment unsolved. In contrast to the one- and two vortex system, it is not even sure whether the final steady state, expected from the numerical results, has already been established. Some (but surely not all) of the additionally singular points have been found and could be defined. It seems that directly on the front and back walls still only one focal point still exists. That means that the topology on these walls remains unchanged. The interior of the cube, however, and in particular the regions close to the axes of the vortices where flow reversal with respect to the y-direction occurs, has not yet been fully analyzed. Therefore, the topological flow pattern proposed in Fig. 5c has only tentative character. Here, more detailed information is needed. The same is true for the embedding of the third vortex into the flow field. On the vertical center plane the aforementioned two vortices are still present, but the v-component of the vortex close to the hot wall has changed its sign.

Discrepancies between the calculations and observations (especially with respect to the flow direction along the axes of the spirals) seem not to be so serious as one would suspect at first. The net motion along a streamline into the y-direction is the result of alternating forward-backward movements. This also holds for the loops of the inner spirals which cross the positive and negative regions of the v components. The velocity distribution in the v-direction on a z-x plane ($y = 0.5$), loosely speaking, has a maximum in the left upper and right lower corners, and a minimum in the two other corners. In the centre of the plane there is a saddle point, and the velocity is zero on the walls. So, a small shift of the spiral axis due to unconvincing values of the fluid properties or deviations from the boundary conditions assumed, may deform the flow field. These speculations are supported by two facts: 1. The observed shape of the vortex axes deviates considerably from the calculated ones, and 2. the experimentally observed isotherms on the x-y planes are considerably shifted in the x-direction into the neighbourhood of the front and back walls ($y = 0.1$) in contrast to the calculated positions. This induced us to reformulate the boundary conditions for the heat flux, a work which is under way. As the numerical code enables us to prescribe the boundary temperature on the inner surfaces, it is planned to repeat the calculations by defining *a priori* the measured temperature distribution for all six walls.

The observed transition from one-vortex to two-vortex and also to three-vortex convection changes the number of critical points, i.e. local topological bifurcations occur [8]. Due to reversal of the direction of streamlines between singularities, global topological structures are also changed. The problem, whether one can define a critical number dividing these different topological structures, could not be solved. From the experimental point of view there are no sharply defined values for the Rayleigh number separating these structures. To answer these open questions there is a need to extend the present study by further experiments and improved numerical simulation.

6 LITERATURE

[1] Mallinson G.D., de Vahl Davis G., Three-dimensional natural convection in a box: a numerical study, J.Fluid Mech., **83**, pp.1-31, 1977.

[2] Kirchartz K.R., Dreidimensionale Konvektion in quaderförmigen Behältern, Habilitationsschrift, Universität Karlsruhe 1988.

[3] Hiller W.J., Koch St., Kowalewski T.A., Three-dimensional structures in laminar natural convection in a cube enclosure, Experimental Thermal and Fluid Scs. 2, 34-44, 1989

[4] de Vahl Davis G., Laminar natural convection in an enclosed rectangular cavity, Int. J. Heat Mass Transfer, **11**, pp. 1675-1693, 1968.

[5] de Vahl Davis G., Finite difference methods for natural and mixed convection in enclosures, Heat Transfer 1982, vol.1, pp. 101-109, Hemisphere, Washington 1982.

[6] Yeah B.P., de Vahl Davis G., Behnia M., Program SOLCON 3D-solidification and convection of a viscous liquid in a box: Users'Manual. UNSW Report (in preparation)

[7] de Vahl Davis G., Convection of air in a square cavity: a bench mark numerical solution. Int. J. Num. Meth. Fluids 3, 249-264, 1983.

[8] Dallmann U., Three-dimensional vortex structures and vorticity topology, Fluid Dyn. Res., 3, pp.183-189,1988.

We are indebted to Peter Baumann from Max-Planck-Institut for his great help in displaying computer generated tracks.

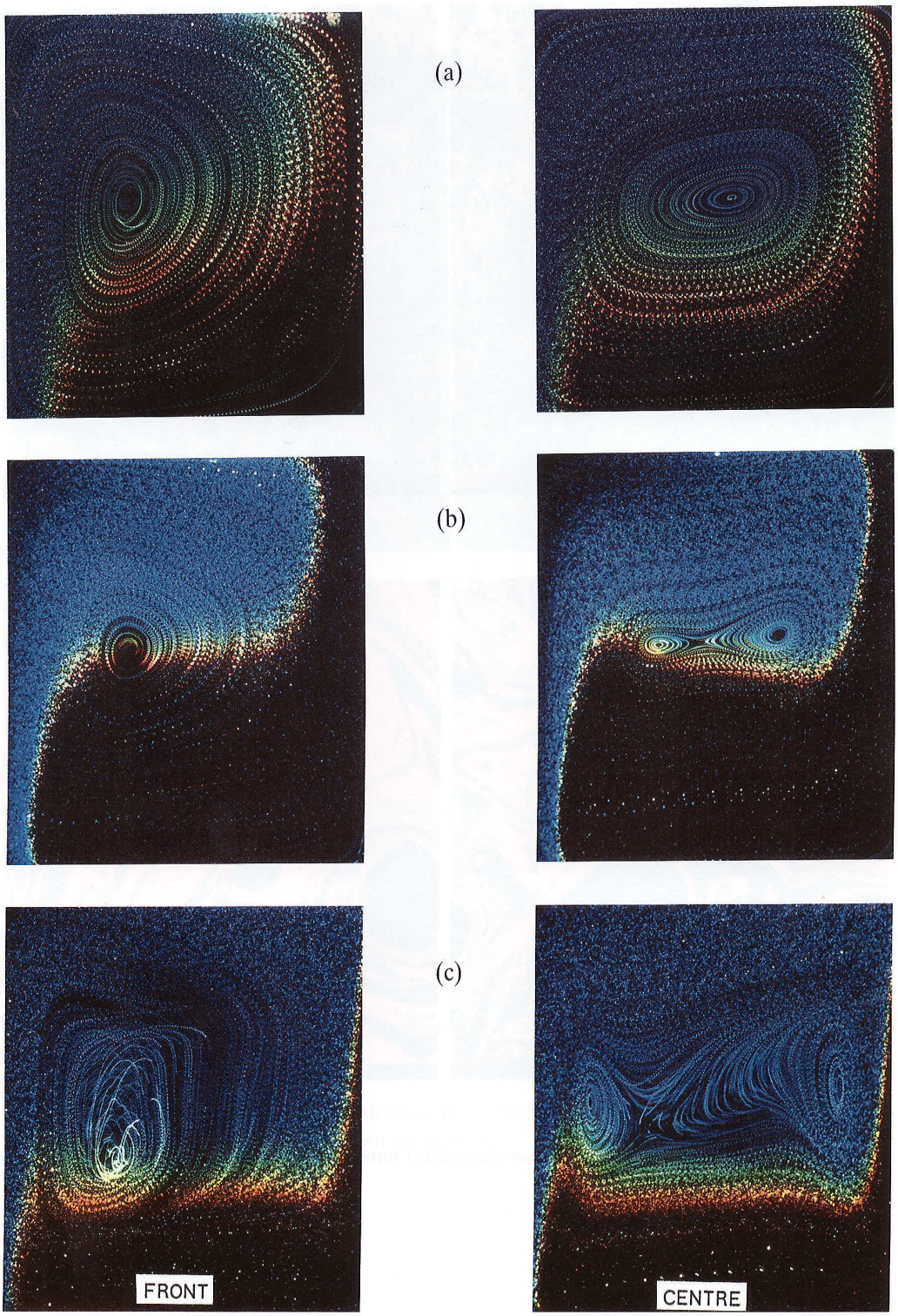

Figure 2 Streamlines in a vertical plane y=0.05 (left) and the flow in the vertical centre plane y=0.5 (right). Left side (z=0) is the hot wall; (a) Ra=2.10^4, Pr=6300; (b) Ra=8.10^4, Pr=6900; (c) Ra=$7.5{\cdot}10^5$, Pr=225. Red colour corresponds to ~27°C, blue to ~29°C.

See page 720.

Plate 12 Symposium Photograph

Symposium Photograph